Authors response

We thank the anonymous referee for the interest in our study and the careful reading which helped to improve the paper. We hope that our replies to the comments answer the issues in a satisfying way, and that the changes in the manuscript motivated by the comments improved the paper. We first list the central changes in the revised version of the manuscript to give an overview. Then we reply to each comment in a point-by-point response and in the following order: 1.) comment from the reviewer, 2.) our response and 3.) the changes in the manuscript. The modified text passages are given in italics.

Central changes in the revised manuscript:

- We changed the map projection in Fig. 2 from Mercator to Plate Carrée, to match the projection of Fig. 7 (respectively Fig. 6 in the previous version of the manuscript). We furthermore adjusted the colors in Fig. 2 to avoid the combination of red and green filled contours.
- Figure 3 in the revised manuscript now includes information on the occurrence of strong vertical wind shear $S^2 \geq S_t^2$.
- We identified an error in the plotting routine for the latitude-altitude crosssections which depict the temporal and zonally averaged occurrence frequencies for strong vertical wind shear. After a carefull revision of the plotting routine we re-created Fig. 4 and Fig. 5a (Fig. 5b in the revised manuscript). We show the changes here below (Fig. 4 and Fig. 5 in this reply). As can be seen, slightly larger values in the TSL occurrence frequencies are now apparent above the local tropopause. Overall, this revision has no effect on the interpretation of our results and the conclusion of our study.
- Figure 5 now includes an additional panel depicting the zonally averaged occurrence frequencies for strong vertical wind shear in absolute height coordinates (Fig. 5a). It furthermore includes a panel which depicts the zonally averaged occurrence frequencies relative to the cold point tropopause in the tropics respectively relative to the $Q = 2$ pvu dynamic tropopause in the extratropics (Fig. 5c). Both changes were motivated by comments from the two referees.
- The schematic of the averaging method (Fig. 5b in the previous version of the manuscript) is now included as an individual figure (Fig. 6 in the revised manuscript).
- Motivated by a comment from one of the referees we repeated each analysis step concerning the occurrence frequencies of strong vertical wind shear near to the tropopause with an adjusted vertical search range around the LRT to make the results more representative for both the tropics as well as the extratropics. The occurrence of strong vertical wind shear near to the tropopause is now defined as $S^2 \geq S_t^2$ at least within one grid box between 1 km below and 2 km above the LRT. Thus, the occurrence frequencies in Fig. 7, 9, 10, 11, 12 and 13a in the revised manuscript are overall slightly larger

(Fig. 6, 8, 9, 10, 11, 12a in the previous manuscript). This does not affect the interpretation of our results and the overall conclusion of this study.

- The horizontal map projections (Fig. 2, 7 and 12 in the revised manuscript) now depict the horizontal wind on the 200 hPa isobaric surface instead of the vertically integrated horizontal wind (Koch et al., 2006). After revising the manuscript we decided that the vertically integrated wind did not add significant information, and the more commonly depicted horizontal wind on an isobaric surface is more easily to interpret.

- We removed the information on the dynamic tropopause in Fig. 11 in the revised manuscript (Fig. 10 in the previous version) because it was not explicitly discussed in the text.

- Figure 13 in the previous version of the manuscript was replaced by Fig. 14 in the revised manuscript. Figure 14a shows a 2d-histogram of the distribution of N^2-S^2 pairs within the first three kilometers vertical distance from the LRT and for the whole ERA5 data set which is analysed in the study. Figure 14b shows the associated distribution of Richardson numbers in this region. These changes were motivated by comments from the referees.

Point-by-point response to the first review

Main comments:

Comment 1: The role of model vertical resolution is acknowledged in several instances but could be discussed more thoroughly. The authors mention in the introduction (p 3 l 67) that the previous generation of ECMWF reanalysis (ERA interim) was unable to describe the shear layers. How much improvement has ERA 5 brought ? The statement that it has 'a sufficient resolution to realistically resolve central features in the UTLS' (p 6 l 167-168) could be justified, although a comparison to radiosonde or other observations might be beyond the scope of this paper. The authors could refer to Figure 1 of Hoffman et al. (2019) which shows the respective resolution of ERA interim and ERA 5.Similarly, on p 6-7 l 197-199, the issue of vertical resolution variations with altitude is raised but its impact is not estimated quantitatively. The authors may want to mention that the change in vertical resolution is slight in the region of interest, a few percent (how many ?) compared to the changes in shear occurrence frequency which varies by 2 orders of magnitude in their Fig. 3.Finally, the authors could briefly comment on the performance of ERA5 compared to the ECMWF operational analysis which they analyzed in Kaluza et al. (2019).

Reply to comment 1: We realize that the additional information on the resolution of the ERA5 is necessary to put the results of the study into context, and have included the proposed changes into the manuscript.

p.5 L160: The goal is to present a consistent area-wide analysis of the vertical and geographic occurrence frequency distribution for strong wind shear in a state of the art long term numerical representation of the atmosphere, i.e., the ERA5 reanalysis. Compared to observational research studies our approach has no spatial limitiations to assess the occurrence frequency. However, for our analysis it is necessary to keep in mind that the vertical wind shear features are only as well represented as the model resolution allows them to be. An important factor in this context is the vertical resolution, which has improved significantly compared to the ERA-Interim reanalysis as a reference dataset (e.g., Hoffmann et al., 2019).

p.7 L205: The increasing vertical grid spacing with increasing altitude in the native coordinates results in a bias towards a larger resolved spectrum of vertical wind shear at lower altitudes, which should be considered. However, the analysis focusses on the UTLS region where the vertical grid spacing increases from about 300 m at 5 km altitude up to about 400 m at 20 km altitude (e.g., Hoffmann et al., 2019). Thus, the resolution bias should not have a large impact on the results presented.

p.15 L352: We expect the ERA5 reanalysis to resolve vertical wind shear features in the UTLS similarly well compared to the operational IFS analysis data used in Kaluza et al. (2019). However, a direct comparison should be made carefully. The ERA5 reanalysis is based on an IFS version with a $T_{\mathrm{L}}639$ spectral truncation (about 31 km horizontal grid spacing, Hersbach et al. (2020)) and 137 vertical level, compared to the $T_{\mathrm{L}}1279$ spectral truncation (about 16 km horizontal grid spacing) and 91 respectively 137 vertical level in the operational analysis data used in Kaluza et al. (2019).

Comment 2: Reading the paper made me wonder how much of the shear structure might be diagnosed/explained using the thermal wind relation (for instance the pattern in Fig. 4 and 5 a, the relationship with ridges in Sect. 4.2 or the seasonal variation of the EAJS in Sect. 4.3.1). The authors emphasize (p 24 l 547) that part of the co-location with the tropopause is related to thermal wind balance, as suggested for example in the cited study by Endlich and McLean (1965). They could test this hypothesis quantitatively. Sure, it does not directly explain how the temperature gradient are generated but this is documented elsewhere and a simple diagnosis could here help disentangle "balanced dynamics" from gravity wave effects.

Reply to comment 2: We thank the reviewer for this suggestion. We started to compare the wind shear based on the full model wind and the thermal (model) wind. We extended the discussion in Sect. 3 to include a comparison of these two metrics based on a single day analysis (Fig.15 in the manuscript, Fig. 1 in the this reply). The comparison shows that there is in general a good agreement in the larger scale in the extratropics, however, with distinct differences which are presumably mainly caused by resolved gravity waves. We have not included a climatological analysis of this comparison. We think that such a comparison would increase the content of this manuscript substantially. Also new metrics would need to be introduced, since the metrics used in this study are not suited for such a comparison. The zonal averaging of occurrence frequencies of $S^2 \geq S_t^2$ as well as the quasi-horizontal mapping of strong wind shear near to the tropopause could show a good agreement between the full model wind shear and the thermal wind shear, even if the thermal wind does not represent the shear regions well, due to a superposition of underestimation and overestimation of the actual wind shear at different longitudes. This is indicated in

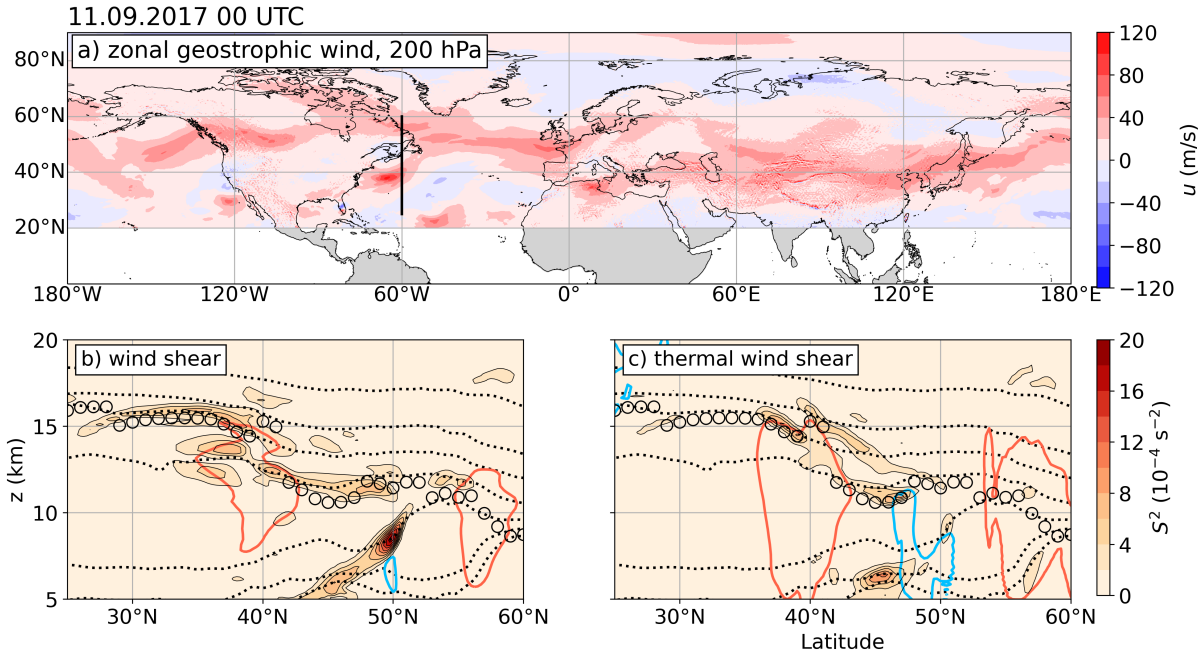

Figure 1. Comparison of the vertical wind shear based on the full model winds and on the thermal wind relation. a) Geostrophic wind at 200 hPa, for the northern hemisphere on 11 September 2017. Regions south of 20° N are left out because the validity of the assumption of geostrophic balance vanishes towards the equator. Black solid line indicates the vertical cross sections in panel b and c. b) Color contour shows vertical shear of the horizontal wind derived from the wind components in the ERA5 data (S^2, in ms^{-2}). Red and blue lines show $u = 30\ \mathrm{ms}^{-1}$ and $u = -10\ \mathrm{ms}^{-1}$ isotachs of the zonal wind. Black dotted lines show isentropes. Black circle markers indicate LRT altitude. c) As in b but for the thermal wind calculated from the temperature field in the ERA5 data. Red and blue lines show $u = 30\ \mathrm{ms}^{-1}$ and $u = -10\ \mathrm{ms}^{-1}$ isotachs of the zonal geostrophic wind.

the exemplary cross sections. We motivate further research on a more general comparison of the TSL with the thermal wind relation at the end of the paragraph.

p.24 L514: The connection between the temperature field and the vertical wind shear for synoptic scale flow can be approximated through the thermal wind relation, i.e., the vertical gradient of the geostrophic wind under the assumption of hydrostatic balance. Figure 14a shows the geostrophic wind at 200 hPa on 11 September 2017, i.e., the date of the exemplary single day analysis in Sect. 3. Overall, the geostrophic wind approximates the synoptic scale flow realistically (compare Fig. 2). However, it overestimates the absolute zonal wind speed in cyclonic rotational systems like the one over the northwest Atlantic, in accordance with the fact that inertial forces are neglected (Holton and Hakim, 2012). The vertical structure of the geostrophic wind is shown exemplarily in the vertical cross sections at 60° W (Fig. 14b and c). The thermal wind relation results in several regions of strong vertical wind shear near to the tropopause. The comparsion with the vertical wind shear derived from the

full model wind reveals a certain degree of agreement, in particular on the synoptic scale, but also differences on the smaller scales. The strength of the vertical wind shear at 40° *N and 15 km altitude is overestimated by the thermal wind approximation, as well as the shear region directly above that reaches north- and downward. The southward extent of the region of strong wind shear on the other hand is underestimated. The two pronounced wind shear regions below the tropopause and south of* 40° *N are not evident in the the thermal wind shear. The geostrophic zonal wind in the upper troposphere at about* 50° *N deviates from the full model zonal wind, which results in a significant underestimation the vertical wind shear below the tropopause. At the same time, the thermal wind relation overestimates the shear region below the tropopause at* 45° *N, which is caused by strong meridional temperature gradients (not shown). The maximum of the thermal wind shear at* 45° *N directly above the LRT is not evident in the full model wind shear, but instead is apparent in a region that is located further to the north. Overall, the comparison indicates the significance of dynamic processes on smaller scales on which other forces than pressure gradient and Coriolis force need to be taken into account (Newton and Persson, 1962). This example already shows that many details, especially related to mesoscale dynamic features, need to be considered to fully address the differences in the vertical wind shear based on the full model winds and on the thermal wind relation. A comprehensive analysis of these differences is beyond the scope of the current study but will be pursued in future work.*

Comment 3: If the resolution of ERA5 is good enough to distinguish the LRT from the cold point tropopause (CPT), it would be interesting that the authors determine which of the LRT or the CPT is closest to the enhanced shear layer in the tropics. This would be particularly relevant to the question of the stratosphere-troposphere boundary in the tropics (e.g. Pan et al., 2018) . I note that, in Fig. 5, the shear layer in the tropics is shifted upward by 1 pixel (500 m) with respect to the LRT.

Reply to comment 3: Motivated by this comment as well as a similar comment by the other reviewer, we have included the vertical distributon of grid volumes with $S^2 \geq S_t^2$ in the 10 year temporal and zonal average in a CPT-relative vertical coordinate for the tropics (Fig. 2c in this reply). It is possible to resolve the different locations of CPT and LRT in the tropics in ERA5. However, the occurrence of strong wind shear appears to be more closely linked to the stratification criterion that defines the LRT. The more pronounced occurrence frequency maximum below the CPT is closely linked to Fig. 13b and c and the related discussion on the frequently occuring lapse rate tropopause jump within the TEJ and the winter easterlies over the maritime continent. The CPT is more often located above the downward sloping regions of strong wind shear.

p.13 L307: The significance of the processes which result in the occurrence of the TSL remains to be quantified. The clustering of grid volumes which exhibit $S^2 \geq S_t^2$ *directly above the LRT in Fig. 5b agrees with the dynamic stability criterion and the thermal wind shear forcing associated with upper tropospheric fronts. However, the overall link between the tropopause definition, which is goverend by the temperature profile, and the occurrence of strong vertical wind shear remains uncertain. Therefore, we repeat the analysis for the tropical cold point tropopause (CPT), i.e., the absolute temperature minimum in the tropical UTLS, and for the dynamic tropopopause, i.e., the* $Q = 2$ *pvu isosurface in the extratropics. The tropics feature a*

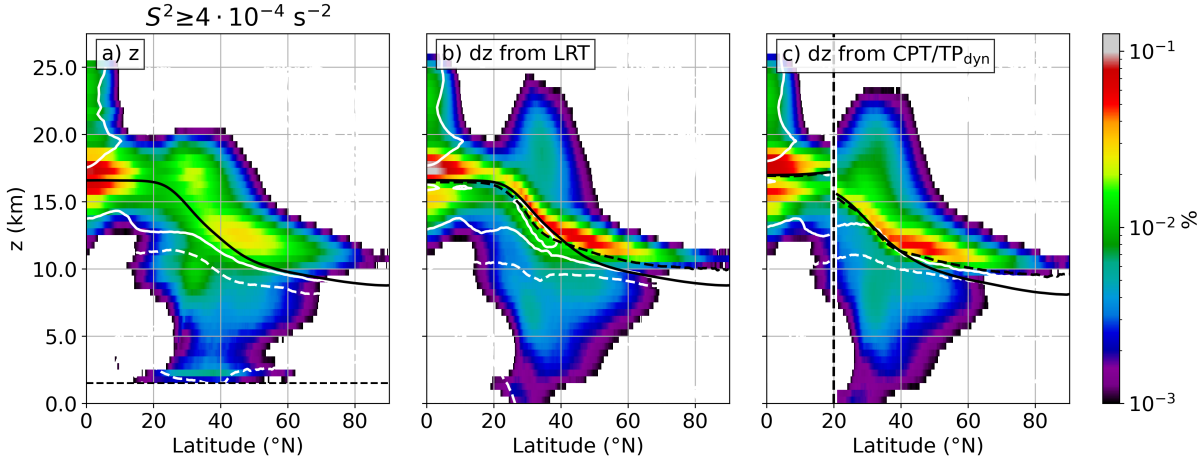

Figure 2. Northern hemispheric occurrence frequency distribution of grid volumes that exhibit strong vertical wind shear $S^2 \geq S_t^2$, from 1 Januaray 2008 to 31 December 2017. Logarithmic frequency contour, vertically binned with $dz = 500$ m. a) Geometric altitude as the vertical coordinate. Solid bold black line indicates mean LRT altitude for all 10 years and the whole northern hemisphere. Dashed thin black line indicates the effect of the 1.5 km above orography cut-off. White solid (dotted) line indicates regions where negative (positive) vertical wind shear makes for 75 % of the counts. b) As in panel a, with LRT-relative vertical coordinate and with mean LRT altitude for profiles with $S^2 \geq S_t^2$ restored (dashed bold black line). Solid bold black line as in panel a. c) As in panel b but from $0° - 20°$ N with the cold point tropopause (CPT) as a reference altitude, and north of $20°$ N with the dynamic tropopause ($Q = 2$ pvu) as a reference altitude.

distinct separation of up to 1 km between the LRT and the CPT (Seidel et al., 2001), which motivates the comparison at low latitudes. The PV on the other hand does not constitute a useful tropopause definition in the tropics (Holton, 1995), which is why the dynamic tropopause is only used in the extratropics in this study. From Fig. 5c it is evident that ERA5 resolves the separation of the LRT and the CPT in the tropics, along with central features like a decreasing mean distance between the two tropopauses towards the equator (Seidel et al., 2001). The clustering of strong wind shear grid volumes above the CPT is less pronounced compared to the LRT, along with a more pronounced secondary maximum below the CPT, which indicates that the occurrence of strong vertical wind shear is more closely linked to the LRT in the tropics.

Other comments:

Comment: p 2 l 30: 'thermodynamic structure' : do you mean because of mixing and heat exchange? If yes, this should be explained. Otherwise, 'dynamic structure' or just 'structure' would fit better (wind shear is strictly speaking not a thermodynamic feature).

Reply to comment: We agree, thank you for the clarification. We changed the wording accordingly.

p.2 L30: The distribution of vertical wind shear in the atmosphere is a substantial feature of the dynamic structure because it controls the dynamic stability of the flow.

Comment: P 3 l 61: Please convert feet to meters, following WCD guidelines.

Reply to comment: Thank you for the hint.

p.3 L60: The data showed distinct occurrence frequency maxima of enhanced values of S^2 within sampling windows of 0.9 km at altitudes of about 9-12 km.

Comment: p 3 l 91: The authors may want to cite the recent paper by Trier et al. (2020). In this paper the occurrence of CAT around a mid-latitude cyclone is investigated with a special emphasis on its relation with gravity waves. This paper would also be relevant in the discussion, with the caveat that the small-scale waves are likely not resolved in ERA 5.

Reply to comment: We greatly appreciate this information, the study by Trier et al. (2020) is very informative and educational, and we agree that it should be referenced in our study.

p.4 L97: Recently, the high resolution numeric simulation of a midlatitude cyclone which was associated with a large number of turbulence reports gave insight on the importance of the tropospheric jet streak and wind speed and shear enhancement within upper tropospheric outflow of deep convection on the occurrence of CAT, along with the generation of gravity waves on different scales and their interaction with the background wind shear profile at critical levels as well as in regions of subcritical Richardson numbers (Trier et al., 2020).

Comment: p 6 line 191 : There is a typo in the definition of Q, with an extra $\times$ which should be removed (the dot is the conventional notation for the scalar product). Also, is it the 'full definition' which is used here, with $\mathbf{\Omega}$ the vector of angular rotation? Although I imagine the differences will be small, I believe it should be replaced by $f\mathbf{k}$ where $\mathbf{k}$ for consistency with the primitive equations solved in the ECMWF model.

Reply to comment: We have corrected the typo in the equation, and we have added the definition of the potential vorticity as a conservation property in the primitive equations.

p.6 L191: Following the definition of Ertel (1942) the potential vorticity (PV) can be written as

$$Q = \frac{1}{\rho}\boldsymbol{\eta} \cdot \boldsymbol{\nabla}\Theta, \tag{1}$$

where ρ is the density of the medium, and $\boldsymbol{\eta} = \boldsymbol{\nabla} \times \boldsymbol{u} + 2\mathbf{\Omega}$ the vector of the absolute vorticity with the angular velocity of the earth $\mathbf{\Omega}$. In the context of the primitive equations which are solved by the IFS this translates to

$$Q = \frac{1}{\rho}(f\boldsymbol{k} + \boldsymbol{\nabla} \times \boldsymbol{u_h}) \cdot \boldsymbol{\nabla}\Theta, \tag{2}$$

where $f = 2\Omega sin(\phi)$ is the Corliolis parameter which represents the component of $\mathbf{\Omega}$ in $\boldsymbol{k}$ direction of the local rectangular coordinate system, and $\boldsymbol{u_h}$ is the vector of the horizontal wind. .

Comment: p6 line 196-197: I guess altitude is retrieved from the geopotential. Maybe state it explicitly.

Reply to comment: That is correct. We have added the according information in the methods description.

p.7 L203: The altitude at each model level is derived from the geopotential after vertically integrating the hydrostatic equation from the pressure and temperature profiles (for further information refer to the IFS documentation, ECMWF (2016)).

Comment: P7 l 211: This paper is submitted within a special issue (WISE) and I guess the field campaign motivated the choice of the date. This could be mentioned here.

Reply to comment: We have added this information.

p.8 L222: This study was performed in the context of the airborne research campaign WISE that took place during SON 2017 over the North Atlantic, which motivated the choice of the date.

Comment: P10 line 251, figure 5a) and related discussion: Could you also show the equivalent of Fig. 4 a) on top of Fig 4c) which is shown here? This would emphasize the relevance of using tropopause relative coordinates and help understand lines 256-258.

Reply to comment: We have included the proposed subfigure along with the analysis relative to the CPT in Fig. 4 in the manuscript, respectively Fig. 2 in the present document.

p.10 L262: Figure 5a shows the 10 year temporal and zonal average occurrence frequency for strong vertical wind shear $S^{\geq} S_t^2$, with the geometric altitude as the vertical coordinate. The mean LRT altitude for the same time period and region is indicated by the black solid line. Three distinct occurrence frequency maxima are apparent, i.e., in the midlatitudes between $40^\circ - 60^\circ$ N and mainly above the LRT, at the tropopause break at about 30° N above and below the LRT, and in the tropics in close vicinity above and below the LRT. The rearrangement of the grid boxes in the LRT-relative vertical coordinate system (Fig. 5b) concentrates the occurrence frequency maxima in a distinct layer above the LRT. This layer spans from the tropics to latitudes north of 60° N, and it exhibits occurrence frequencies of the order of $1\,\%$–$10\,\%$ over a vertical range of about $1-2$ km.

Comment: p 13 line 305-306 and Fig. 6: Do you know how exactly this surface is defined in the ECMWF ? In particular, I am surprised that the PV=2 PVU surface crosses the equator in Fig. 6. If there is some adjustment at low latitudes in the ECMWF field it would be useful to mention it here.

Reply to comment: The dynamic tropopause provided by the ECMWF is defined as the $Q = 2$ pvu isosurface or the 96 hPa if $Q = 2$ pvu is located at lower atmospheric pressure. We have now excluded the dynamic tropopause information for trop-

ical latitudes throughout the manuscript to prevent misconceptions, since the "dynamic tropopause in the tropics" was never directly used in the analysis.

Comment: P 18 l 384: low $\longrightarrow$ lower . 40 m/s is not a particularly low wind speed even compared to the subtropical or eddy-driven jet.

Reply to comment: You are correct. Nevertheless, our intent was to emphasize that frequent strong wind shear is not necessarily linked to large jet core wind speeds. We have changed the phrasing and added a reference to the STJ core speeds identified by Wu and Sun (2017).

p.20 L440: They exhibit a limited vertical extent and maximum wind speeds around 40 ms^{-1}, which is low e.g. compared to the EAJS core speeds identified by Wu and Sun (2017))..

Comment: P 18 l 391: I am not sure how the geographic distribution here can be compared with the radiosondes from 2 stations in Sunilkumar et al. (2015). Agreed, the stations are influenced by the TEJ but from two points it seems complicated to validate a geographic pattern. A slight difference is that S2015 see this increase above the monthly mean CPT (their fig. 4), which might be 600 m (2-3 ERA5 levels) above the lapse rate (Sunilkumar et al., 2013; Munchak and Pan, 2014). Given the depth of the layer (1 km) used by the authors to investigate shear in tropopause relative coordinates, 600 m is significant. See also main comment 3.

Reply to comment: We agree that this sentence was misleading. We reversed the sentence to make the statement more clear. The intention was to put the results in context with observational studies in this region, since the occurrence frequency maximum over the Indian Ocean is very striking and the occurrence of strong shear is not directly intuitive. Concerning the second part of your comment, we agree that the TSL depth of 1 km was set to low to investigate the geographic mapping of strong wind shear above the LRT, particularly in the tropics. We changed the search radius for the criterion of strong wind shear occurrence near to the tropopause to the region from 1 km below the LRT to 2 km above. This applies to all analysis steps throughout the manuscript. This change has no implications on the interpretation of any of the results, only the occurrence frequencies are generally shifted towards slightly larger values, particularly in the tropics. Thus, the analysis is more consistent.

p.20 L446: Furthermore, the occurrence frequencies for strong vertical wind shear which were derived from radiosonde measurements by Sunilkumar et al. (2015) agree qualitatively with the ones at the respective geographic location of each radiosonde station in Fig. 7c.

Comment: p 19 l 409 : Could you provide the correlation coefficient ?

Reply to comment: We have included the correlation coefficient.

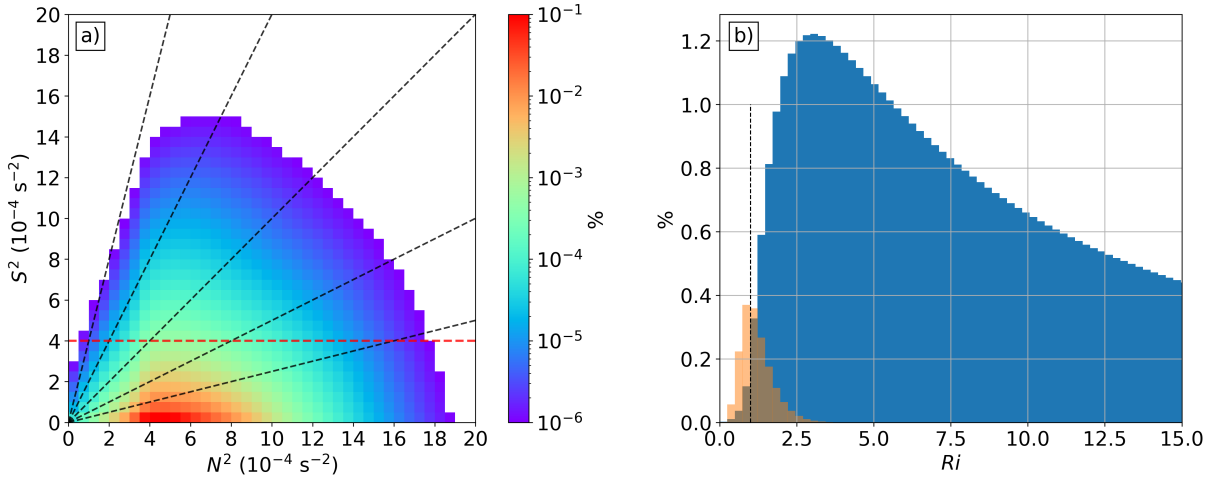

Figure 3. a) Relative occurrence frequency distribution of N^2-S^2 pairs in the region between the LRT and 3 km above, for all daily northern hemispheric ERA5 fields from 2008-2017. Logarithmic occurrence frequency color scale. Red dashed line indicates $S^2 = S_t^2$. Dashed black lines indicate the Richardson numbers 0.25, 0.5, 1.0 ,2.0 and 4.0. b) Histogram of the relative distribution of Richardson numbers associated with the data displayed in panel a. Orange bars show Ri for grid volumes with $S^2 \geq S_t^2$, and blue bars for the remaining grid volumes between the LRT and 3 km above. Dotted black line indicates $Ri = 1$.

p.22 L466: The comparison of these time- and area-averaged frequencies with the Oceanic Niño sea surface temperature anomaly Index values for DJF (ONI) show an anticorrelation (Fig. 13a), with a Pearson correlation coefficient of $r = -0.788$.

Comment: P 20 l 410: 'neutral and La Nina conditions': do you mean ' neutral and El Nino conditions'?

Reply to comment: The time and area averaged occurrence frequencies maximise along with negative ONI values which indicate la Niña phases.

Comment: P 20 l 440: you might consider showing a scatter plot of N2 and S2 to demonstrate this

Reply to comment: We agree that this statement concerning the non-correlation of N^2 and S^2 needs to be substantiated. The discussion section now includes such a 2d-histogram (Fig 3a in the present document, Fig. 14a in the manuscript), along with the according discussion. This figure is also used in the subsequent discussion on the occurrence of comparatively low Richardson numbers in the lower stratosphere.

p.23 L499: Figure 14a shows the relative occurrence frequency of N^2-S^2 *pairs for all ten years and in the region between the LRT and 3 km above. The majority of grid volumes exhibit a static stability between the stratospheric background* $\overline{N^2}_{strat.} = 4 \cdot 10^{-4}$ s^{-2} *and moderately enhanced values associated with the TIL. At the same time, comparatively "weak" vertical wind shear* $S^2 < 4 \cdot 10^{-4}$ s^{-2} *is most prevalent. Vertical wind shear and static stability do not correlate, and enhanced*

values of S^2 can be found within a large spectrum of N^2 under the condition that dynamic stability $Ri > Ri_c$ is (for the most part) maintained. Particularly the largest values of N^2 and S^2 do not correlate..

Comment: p 21 l 450: you might note that ERA 5 has been shown to represent realistically part of the gravity wave activity (e.g., Krisch et al., 2020; Podglajen et al., 2020), which justifies that Gws might indeed be responsible for the enhanced shear in the reanalysis.

Reply to comment: Thank you for referencing these research studies, they helped to put the results better into context. We cited both studies in the discussion section, along with the recent research study on vertical wind shear in the IFS and the UTLS region by Schäfler et al. (2020).

p.24 L539: Recently, Podglajen et al. (2020) compared long-duration superpressure balloon measurements with Lagrangian trajectories calculated from a set of numerical reanalysis products, and where able to show that the ERA5 reanalysis resolves central features of the gravity wave spectrum. The underlaying IFS model resolves low frequency large scale gravity waves down to wavelengths which approach the effective resolution, which is generally estimated to exhibit a factor of about 10 compared to the effective grid spacing. The assimilation of high resolution observational data further enhances the gravity wave activity in the model, which likely involves generation processes and gravity wave scales that are not resolved in the IFS. Furthermore, Krisch et al. (2020) identified individual wave packets in the ERA5 data that had been observed with the Gimballed Limb Observer for Radiance Imaging of the Atmosphere (GLORIA) during the GW-LCYCLE airborne measurement campaign. While these studies confirm that modern reanalysis products are capable to resolve central features of the gravity wave spectrum, the overall vertical wind variability due to gravity waves is likely still underestimated in the ERA5. Recently, Schäfler et al. (2020) reported a significant underestimation of the vertical wind shear near to the tropopause in the IFS, based on a comparison of Doppler wind lidar measurements with IFS analysis and forecast data. The analysis and forecast errors were most prominent at elevated tropopause altitudes above upper tropospheric ridges, i.e., regions that contribute significantly to the occurrence of the TSL in the extratropics. To put these results into context, the model version used by Schäfler et al. (2020) exhibits a spectral truncation of TCo1280 on 137 vertical level, thus, the same vertical grid spacing compared to the ERA5 as well as a larger horizontal resolution.

Comment: p 21 l 459 and fig. 13: for comparison, you could depict the distribution of Ri for all values of shear in the same region as well as the distribution over a deeper layer, to determine whether or not the TIL is a region of low Ri number

Reply to comment: Such a histogram is now included in panel b of Fig. 14 in the manuscript (Fig. 3b in the present document). It supports the remarks that are made in the discussion section concerning the dynamic stability in the lower stratosphere in general and in the TSL.

p.25 L557: The grid volumes with $S^2 < 4 \cdot 10^{-4}\ \mathrm{s}^{-2}$ in Fig. 14a are mostly located below the diagonal dashed black line which indicates Richardson numbers of $Ri = 1$. The corresponding relative distribution of Richardson numbers is shown in

Fig. 14b. The distribution peaks at $Ri = 3$ and spans over a large spectrum of larger Richardson numbers (only a section of the distribution is displayed). Richardson numbers of $Ri < 1$ are rarely associated with vertical wind shear $S^2 < 4 \cdot 10^{-4}\ \mathrm{s}^{-2}$. This indicates that the lowermost stratosphere up to 3 km above the LRT is dynamically stable in the absence of strong vertical wind shear. In contrast, a significant proportion of grid volumes which exceed S_t^2 in Fig. 14a are located above the $Ri = 1$ isoline. These grid volumes constitute the greater part of Richardson numbers $Ri < 1$ within the first 3 km above the LRT, which is indicated in Fig. 14b.

Typos and suggested reformulations:

Comment: p 2 l 30: "an substantial" $\longrightarrow$ a substantial

Reply to comment: Done.

Comment: p 2 l 37: 'linear wave theory' $\longrightarrow$ 'linear theory'

Reply to comment: Done.

Comment: p 6 l 185 : I think it is the pressure velocity ω rather than w which is provided by ECMWF.

Reply to comment: Yes, thank you for the hint. We changed the variable name accordingly.

Comment: P10 l 255 : 'compare e.g.' $\longrightarrow$ 'compare with'

Reply to comment: Done.

Comment: p 13 l 298 : 'barclinic'

Reply to comment: Done.

Comment: p 24 l 547: 'fulfils' $\longrightarrow$ 'fulfills'

Reply to comment: Done.

Comment: p 18 legend of Fig. 11: "destails"

Reply to comment: Done.

Comment: p 22 l 467: "e.g." should be before the reference

Reply to comment: Thank you for pointing out the error.

Comment: p 24 l 544: I would remove 'exceptionally' since your analysis shows that this feature is not an exception

Reply to comment: We agree. We changed the phrasing thoughout the manuscript, also motivated by a similar comment by the other reviwer.

Comment: p 24 l 552 : operational analysis $\longrightarrow$ ERA 5

Reply to comment: Yes indeed, thank you!

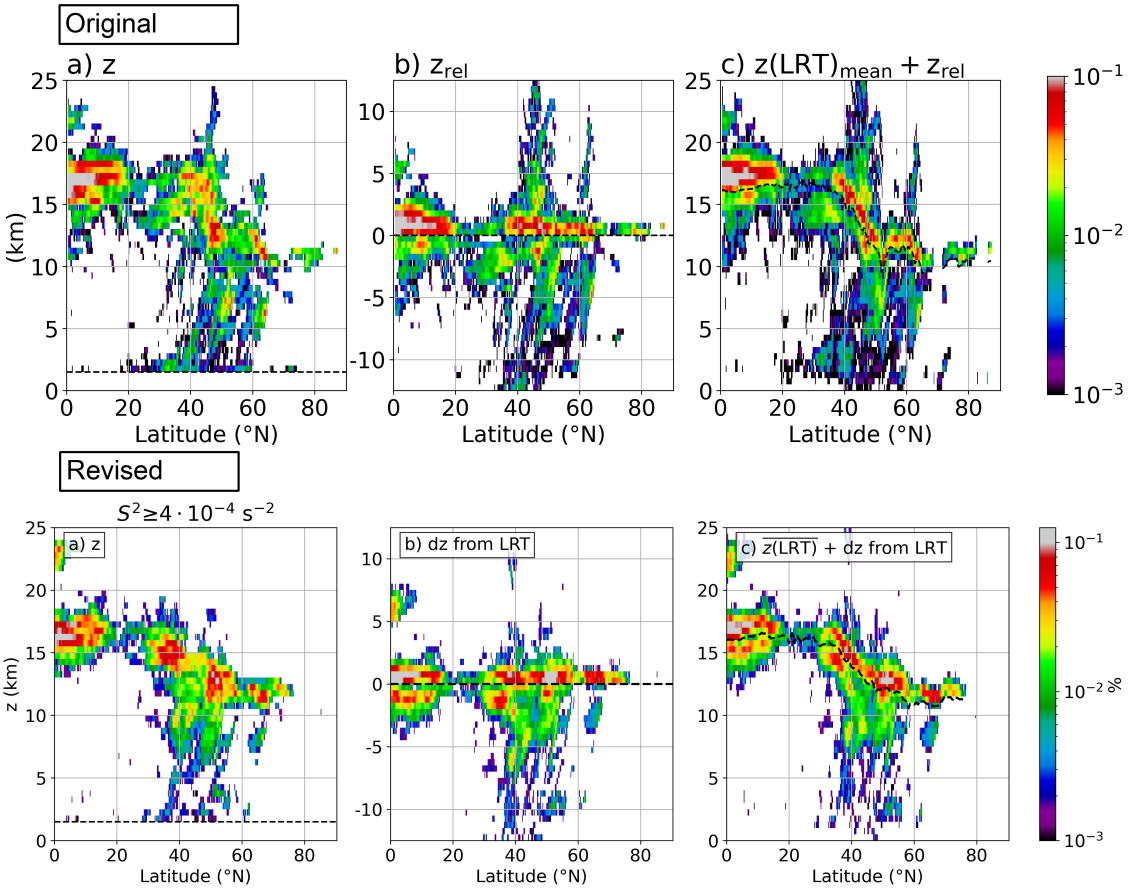

Figure 4. Comparison of Fig. 4 in the originally uploaded manuscript (top row) and the equivalent in the revised manuscript (bottom row). The colorbars had to be extended slightly at the top end due to the larger maximum values, however, with the same colors in the frequency range of $10^{-3} - 10^{-1}$.

References

ECMWF, a.: IFS documentation – Cy41r2 Operational implementation 8 March 2016 Part III : Dynamics and numerical procedures, 2016.

Ertel, H.: Ein neuer hydrodynamischer Erhaltungssatz, Die Naturwissenschaften, 30, 543–544, https://doi.org/10.1007/BF01475602, 1942.

Hersbach, H., Bell, B., Berrisford, P., Hirahara, S., Horányi, A., Muñoz-Sabater, J., Nicolas, J., Peubey, C., Radu, R., Schepers, D., Simmons, A., Soci, C., Abdalla, S., Abellan, X., Balsamo, G., Bechtold, P., Biavati, G., Bidlot, J., Bonavita, M., De Chiara, G., Dahlgren, P., Dee, D., Diamantakis, M., Dragani, R., Flemming, J., Forbes, R., Fuentes, M., Geer, A., Haimberger, L., Healy, S., Hogan, R. J., Hólm, E., Janisková, M., Keeley, S., Laloyaux, P., Lopez, P., Lupu, C., Radnoti, G., de Rosnay, P., Rozum, I., Vamborg, F., Villaume, S., and Thépaut, J. N.: The ERA5 global reanalysis, Quarterly Journal of the Royal Meteorological Society, pp. 1–51, https://doi.org/10.1002/qj.3803, 2020.

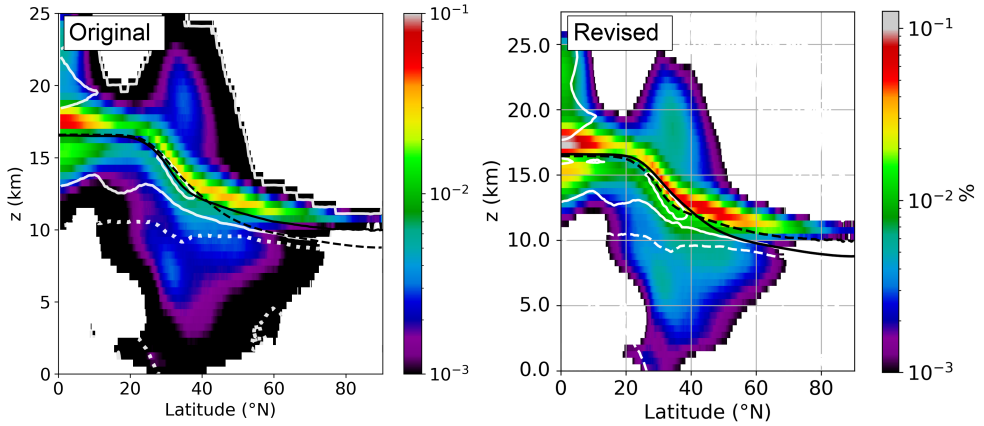

Figure 5. Comparison of Fig. 5a in the originally uploaded manuscript (left panel) and the equivalent in the revised manuscript (right panel). The colorbars had to be extended slightly at the top end due to the larger maximum values, however, with the same colors in the frequency range of $10^{-3} - 10^{-1}$.

Hoffmann, L., Günther, G., Li, D., Stein, O., Wu, X., Griessbach, S., Heng, Y., Konopka, P., Müller, R., Vogel, B., and Wright, J. S.: From ERA-Interim to ERA5: The considerable impact of ECMWF's next-generation reanalysis on Lagrangian transport simulations, Atmospheric Chemistry and Physics, 19, 3097–3214, https://doi.org/10.5194/acp-19-3097-2019, 2019.

Holton, J. R.: Stratosphere–Troposphere Exchange, Stratosphere Troposphere Interactions, pp. 331–355, https://doi.org/10.1007/978-1-4020-8217-7_8, 1995.

Holton, J. R. and Hakim, G. J.: An introduction to dynamic meteorology: Fifth edition, vol. 9780123848, https://doi.org/10.1016/C2009-0-63394-8, 2012.

Kaluza, T., Kunkel, D., and Hoor, P.: Composite analysis of the tropopause inversion layer in extratropical baroclinic waves, Atmospheric Chemistry and Physics, 19, 1–22, https://doi.org/10.5194/acp-2018-1100, 2019.

Koch, P., Wernli, H., and Davies, H. C.: An event-based jet-stream climatology and typology, International Journal of Climatology, 26, 283–301, https://doi.org/10.1002/joc.1255, 2006.

Krisch, I., Ern, M., Hoffmann, L., Preusse, P., Strube, C., Ungermann, J., Woiwode, W., and Riese, M.: Superposition of gravity waves with different propagation characteristics observed by airborne and space-borne infrared sounders, Atmospheric Chemistry and Physics, 20, 11 469–11 490, https://doi.org/10.5194/acp-20-11469-2020, 2020.

Newton, C. W. and Persson, A. V.: Structural characteristics of the subtropical jet stream and certain lower-stratospheric wind systems, Tellus, 14, 2, https://doi.org/10.3402/tellusa.v14i2.9542, 1962.

Podglajen, A., Hertzog, A., Plougonven, R., and Legras, B.: Lagrangian gravity wave spectra in the lower stratosphere of current (re)analyses, Atmospheric Chemistry and Physics, 20, 9331–9350, https://doi.org/10.5194/acp-20-9331-2020, 2020.

Schäfler, A., Harvey, B., Methven, J., Doyle, J. D., Rahm, S., Reitebuch, O., Weiler, F., and Witschas, B.: Observation of jet stream winds during nawdex and characterization of systematic meteorological analysis errors, Monthly Weather Review, 148, 2889–2907, https://doi.org/10.1175/MWR-D-19-0229.1, 2020.

Seidel, D. J., Ross, R. J., Angell, J. K., and Reid, G. C.: Climatological characteristics of the tropical tropopause as revealed by radiosondes, Journal of Geophysical Research Atmospheres, 106, 7857–7878, https://doi.org/10.1029/2000JD900837, 2001.

Sunilkumar, S. V., Muhsin, M., Parameswaran, K., Venkat Ratnam, M., Ramkumar, G., Rajeev, K., Krishna Murthy, B. V., Sambhu Namboodiri, K. V., Subrahmanyam, K. V., Kishore Kumar, K., and Shankar Das, S.: Characteristics of turbulence in the troposphere and lower stratosphere over the Indian Peninsula, Journal of Atmospheric and Solar-Terrestrial Physics, 133, 36–53, https://doi.org/10.1016/j.jastp.2015.07.015, 2015.

Trier, S. B., Sharman, R. D., Muñoz-Esparza, D., and Lane, T. P.: Environment and Mechanisms of Severe Turbulence in a Midlatitude Cyclone, Journal of the Atmospheric Sciences, 77, 3869–3889, https://doi.org/10.1175/jas-d-20-0095.1, 2020.

Wu, S. and Sun, J.: Variability in zonal location of winter East Asian jet stream, International Journal of Climatology, 37, 3753–3766, https://doi.org/10.1002/joc.4947, 2017.